

Spectral imaging using a commercial color-filter array digital camera

Roy S. Berns

Lawrence A. Taplin

Mahdi Nezamabadi

Mahnaz Mohammadi

Yonghui Zhao

Munsell Color Science Laboratory

Chester F. Carlson Center for Imaging Science

Rochester Institute of Technology

54 Lomb Memorial Dr.

Rochester, NY 14623

USA

berns@cis.rit.edu

<http://art-si.org/>

Abstract

A multi-year research program is underway to develop and deliver spectral-based digital cameras for imaging cultural heritage at the National Gallery of Art, Washington DC and the Museum of Modern Art, New York. The cameras will be used for documentation, production imaging, and conservation science. Three approaches have undergone testing: a liquid-crystal tunable filter (LCTF) coupled with a monochrome camera, a six-position filter wheel containing absorption filters coupled with a monochrome camera, and a two-position filter slider containing absorption filters coupled with a color-filter array (CFA) color camera. The last approach is the most practical as it uses conventional digital photography methodologies and equipment and can easily be incorporated into existing museum workflows. A virtual camera model was created that predicted camera signals

from incident radiation and was used to design a pair of absorption filters. The filters were fabricated and tested using a commercial CFA digital camera. Our first experiments have been very promising: Average accuracy was under 1 CIEDE2000 and about 1.5% RMS for both calibration and verification data. This level of performance was superior to our other, more complex approaches.

Key words: spectral imaging, digital photography, color management, cultural heritage digital archiving

Introduction

Imaging is an important technique in the scientific examination of art. Its main use has been for visual documentation. Photographs have long been used to document condition before and after transit, microscopic examinations, conservation treatments, and so on. They are used to enable color reproductions in books and via the Internet. Images using materials with spectral sensitivities in non-visible regions of the electromagnetic spectrum such as infrared and X-ray are equally important to the visible spectrum. Although images are used to record scientific examinations, they are used infrequently as an analytical tool. That is, the amount of colorant in a photographic material would be used to relate to physical properties of the art. In contrast, astronomy, remote sensing, and medicine have exploited this capability for many years. The advent of digital imaging offers increased opportunities to exploit images for the scientific examination of art.

A research program is underway at Rochester Institute of Technology to develop an image acquisition system that records reflection information as a function of wavelength (Berns 2004C, 2004D; Imai 1998, 2000A, 2000B, 2002). Three techniques have been evaluated. The first combines a monochrome area-array camera with a liquid-crystal tunable filter, resulting in a 31-channel imaging spectrometer. The second technique combines the same type of camera with a filter wheel containing six absorption filters; using appropriate color targets and mathematical transformations, spectral images are estimated from the six channels. The third technique uses a color-filter array camera and

a pair of absorption filters, also yielding six channels; the same approach is used to estimate spectral data as the six-position filter wheel. This last technique holds great promise because commercial professional-quality digital cameras can be used. This method was tested using a Sinarback 54H.

Equipment

A Sinarback 54H digital camera back coupled with a Sinar M shutter, P3 body, and 105 mm HR lens were used in this experiment. Sinar CaptureShop 4.1 controlled its operation. This camera incorporates a Kodak KAF-22000CE sensor with a resolution of 5440 x 4080 pixels. The “four-shot” mode was used resulting in 5440 x 4080 non-interpolated RGB data. The cameraback was modified by replacing its infrared cover glass with clear glass. The nominal spectral sensitivities of the sensor are plotted in Figure 1. A pair of Broncolor F1200 HMI lights were used. They produced a correlated color temperature of 4966 K and an illuminance of 9300 lx at the object plane.

Seven targets were evaluated: the GretagMacbeth ColorChecker DC, the GretagMacbeth ColorChecker, the ESSER TE221 scanner target, a custom target of Gamblin conservation colors, an acrylic-medium blue target with a number of different blue pigments, and two small oil paintings. They were used in different combinations as calibration and verification data. For the virtual camera model, a Macbeth XTH integrating sphere spectrophotometer was used (380 – 750 nm); for the imaging experiments, a Macbeth SpectroEye spectrophotometer was used (380 – 730 nm) to measure the spectral reflectance factor of each target.

Virtual Camera Model

A virtual camera model was created in order to select sets of glass filters, shown by Eq. (1):

$$\mathbf{S}_{\lambda,i} = \mathbf{F}_{\lambda} \mathbf{I}_{\lambda} \mathbf{C}_{\lambda,i} \quad (1)$$

where λ is wavelength, ranging from 380 - 750 nm at 10 nm intervals, $\mathbf{C}_{\lambda,i}$ is the spectral

sensitivity of the camera for the i th channel at each wavelength, I_λ and F_λ are spectral transmittances of IR cut-off and glass filters, respectively, and $\mathbf{S}_{\lambda,i}$ is the resulting spectral sensitivity for the entire camera system. For an object with reflectance factor, R_λ , a camera signal, D_i , is calculated by Eq. (2):

$$\mathbf{D}_i = \sum_{\lambda=380}^{750} (R_\lambda \cdot L_\lambda \cdot \mathbf{S}_{\lambda,i}) + n_i \quad (2)$$

where L_λ is the relative spectral power distribution of the illuminant, and n_i is a noise term.

Spectral reflectance is estimated from camera signals by a matrix transformation:

$$\hat{\mathbf{R}} = \mathbf{M}_s \mathbf{D} \quad (3)$$

where $\hat{\mathbf{R}}$ is the $(\lambda \times 1)$ vector of estimated reflectances, \mathbf{D} is a $(i \times 1)$ digital count vector, and \mathbf{M}_s is the $(\lambda \times i)$ transformation matrix (subscript s represents spectral). The transformation matrix was derived using 2,500 virtual pixels and the measured spectral reflectance for each sample of a calibration target; a generalized pseudo inverse calculation incorporating singular value decomposition was used to calculate the matrix. Finally, tristimulus values, \mathbf{T} , a (3×1) vector, are calculated from estimated spectra:

$$\mathbf{T}_s = \mathbf{A}' \hat{\mathbf{R}} \quad (4)$$

where \mathbf{A} is a $(\lambda \times 3)$ matrix of ASTM tristimulus weights.

The Schott filter glass catalog was used to create a set of possible filters. Filters could be single pieces of glass at 1 – 4 mm thickness or “sandwiches” of 1 and 3 mm or 2 and 2 mm. Beer’s Law and the Fresnel equations were used to create these sandwiches. There were 2,830 theoretical filters. Since the camera system would use two filters sequentially, the number of filter pair combinations became 2,831,010. Based on initial noise-free calculations, throughput considerations, and spectral accuracy, the number of candidate combinations was reduced to 30,000.

Using the Esser target as the calibration target, all 30,000 filter sets were tested. That is, Eqs. (1) and (2) were used to create a six-channel digital image. The image and measured

spectral reflectance data were used to derive a transformation matrix. Finally Eq. (3) was used to estimate spectral reflectance for the calibration and verification targets. For example, the relationship between spectral and colorimetric accuracy is plotted in Figure 2.

Twenty-five filter pairs were selected based on their spectral and colorimetric accuracy and spectral transmittance. These were analyzed in detail. One pair was selected for fabrication and experimentation.

Experimental

The spectral sensitivities and the opto-electronic conversion function (OECF) of the camera were measured according ISO standards, 14524 (1999) and 17321 (2003). The normalized spectral sensitivities of the modified Sinar 54 are plotted in Figure 3. These filters are sampling the visible spectrum unevenly; three of the filters have their peaks in wavelength locations well suited for colorimetric imaging, 450 nm, 550 nm, and 600 nm. A metric for colorimetric accuracy, μ -factor (Vora 1993), was calculated for both the six-channel and “production” three-channel camera for several combinations of taking and rendering illuminants. A μ -factor of unity corresponds to perfect color accuracy, only achievable when the camera’s spectral sensitivities are linearly related to CIE color-matching functions and the taking and rendering illuminants are identical. For high-accuracy color imaging, we seek cameras with μ -factor above 0.9. The production camera was made by using a single blue-green absorption filter with very similar spectral properties to that of the removed cover glass. For the production camera, values ranged between 0.68 and 0.85; these values are typical for CFA cameras. The modified camera resulted in higher potential color accuracy; μ -factor increased in all tested cases. An interesting result was that the six-channel camera had higher values than the colorimetric camera when taking and rendering illuminants were unmatched. Increasing the number of channels improved the colorimetric robustness. These calculations also indicate the importance of illumination spectral power distribution on color accuracy.

Images were taken of a uniform gray background, the ColorChecker DC (the calibration target), and the ColorChecker (the verification target) using both the modified and production camera. All the images were digitally flat fielded using the gray background. Three one-dimensional look-up tables were derived that converted encoded digital data to linear photometric data based on the measured OECF. Using the same technique described for the virtual camera, a transformation was derived for the modified camera that estimated spectral reflectance from the post-LUT camera signals.

For both systems, a further colorimetric transformation was derived that consisted of a matrix converting camera signals to tristimulus values, \mathbf{T} , and a second photometric correction, \mathbf{Q} , commonly used to characterize CRT displays (Berns 2000C):

$$\mathbf{T}_c = \mathbf{M}_c \mathbf{Q} \quad (5)$$

$$\mathbf{Q}_i = [k_{g,i} (D_i/D_{\max}) + k_{o,i}]^{\gamma_i} \quad (6)$$

Differences in surface characteristics between the OECF and color-calibration targets necessitated the second photometric correction. Nonlinear optimization was used to derive \mathbf{M}_c and the $k_{g,i}$, $k_{o,i}$, and γ_i coefficients where the objective function was minimizing both the average and maximum CIEDE2000 for the calibration target. For the modified camera, \mathbf{M}_c was a (3 x 6) matrix; for the production camera, \mathbf{M}_c was a (3 x 3) matrix.

For the modified camera, Eq. (5) often results in greater color accuracy than Eq. (4) due to the nonlinear optimization. Using parametric decomposition (Fairman 1997), the estimated spectra were adjusted to achieve the same tristimulus values as obtained using nonlinear optimization:

$$\hat{\mathbf{R}}_c = \mathbf{A}(\mathbf{A}'\mathbf{A})^{-1}\mathbf{T}_c + (\mathbf{I} - \mathbf{A}(\mathbf{A}'\mathbf{A})^{-1}\mathbf{A}')\hat{\mathbf{R}} \quad (6)$$

where \mathbf{I} is an identity matrix.

Results and Discussion

The imaging performance for both the calibration and verification targets is compiled in Tables II - IV. The average colorimetric performance for the production Sinar was quite reasonable for a color managed digital camera (Table II). The nonlinear optimization technique was an effective technique to profile the camera. However, the maximum errors were large. The inherent limitations of the sensor's spectral sensitivities limited performance, consistent with the data shown in Table I.

The modified six-channel Sinar was used to estimate spectral reflectance based on Eq. (4), the performance listed in Table III. Average spectral fit was 1.6% RMS over the spectral range of 380 – 730 nm. Given the inherent constraints of the CFA's spectral sensitivities and the extent of modification by a pair of colored filters, these results were very good. The colorimetric accuracy was similarly high. However, for the calibration data, the maximum colorimetric error was large. Optimizing average spectral accuracy does not lead to optimal colorimetric performance.

Combining the spectral and colorimetric transformations, Eq. (6), resulted in excellent performance, as shown in Table IV. Both average and maximum errors are small. The spectral fits for the ColorChecker are plotted in Figure 4. As a comparison, we have used a monochrome sensor coupled with a liquid-crystal tunable filter to capture 31-band images (Berns 2004D). The average performance for the ColorChecker was $1.5 \Delta E_{00}$ and 1.4% RMS (over the spectral range of 400 – 700 nm). Liang (2004) tested a 13-channel system using a monochrome sensor and interference filters; the average results for the ColorChecker was $1.2 \Delta E_{00}$ and 1.4% RMS (over the spectral range of 400 – 700 nm) using interpolation to transform the multi-channel signals to spectral reflectance. The modified Sinar was able to achieve equivalent performance compared with considerably more complex technologies.

As a final analysis, the transformation vectors from camera signals to spectral reflectance, \mathbf{M}_s , are plotted in Figure 5. The absolute scalar magnitude indicates which filter has the

dominant influence on estimating spectral reflectance at a given wavelength. The goal is to have an appreciable signal for at least one channel at every wavelength. With the exception of 380, 390, and 680 nm, this goal was achieved. By definition, these vectors are affected by the spectral properties of the calibration target. It should be possible to improve these wavelengths by a more optimal calibration target, a current research topic (Mohammadi 2004).

Conclusions

A high-resolution, medium format, production color-filter-array (CFA) digital camera, the Sinar 54H, was modified to facilitate spectral imaging. Modifications included replacing the IR filter with clear glass and fabricating a pair of filters that when positioned sequentially, resulted in six channels sampling the visible spectrum between about 390 and 760 nm. Transformations were derived enabling both spectral estimation and high-accuracy colorimetric imaging. The accuracy achieved equaled or exceeded much more complex imaging systems.

This approach offers numerous advantages. This type of camera is very familiar to museum-imaging professionals. Thus, spectral-based imaging can be readily incorporated into the museum imaging workflow, greatly improving efficiency by eliminating visual editing. Scientific imaging can be the providence of the imaging department rather than requiring the resources of a conservation scientist with color imaging expertise. Since only two images are captured, image registration is straightforward, often a limiting factor in achieving efficiency, for example Liang (2004) and Ribés (2004). If commercialized, the multi-filter CFA camera can produce both color-managed RGB and spectral master images. The RGB images can be used to create derivative images for web-based display and for on-demand and catalog printing. The spectral image can be used for conservation science, lighting design by rendering the image under various lighting conditions (Berns 2002D), and future pedantic research. In conservation, the spectral image can be used as an aid in inpainting (Berns 2002A, 2002B) and pigment identification (Liang 2004), for documenting long-term color changes (Saunders 1993),

digital rejuvenation (Berns 2004A, 2004B), and pigment mapping (Baronti 1998), among others.

Acknowledgements

This research was supported by the Andrew W. Mellon Foundation, the National Gallery of Art, Washington, DC, the Museum of Modern Art, New York, and Rochester Institute of Technology.

References

Baronti, S., Casini, A., Lotti, A., and Porcinai, S. 1998. Multispectral imaging system for the mapping of pigments in works of art by use of principal-component analysis. *Applied Optics* 37, 1299-1309.

Berns, R. S., Krueger, J., and Swicklik, M. 2002a. Multiple pigment selection for inpainting using visible reflectance spectrophotometry. *Studies in Conservation* 47, 46-61.

Berns, R. S., and Imai, F. H. 2002B. The use of multi-channel visible spectrum imaging for pigment identification. Preprints of the 13th Triennial Meeting of the ICOM Committee for Conservation, ICOM, Rio de Janeiro, 217-222.

Berns R. S. and Katoh, N. 2002C. Methods for characterizing displays. in Green, P. and MacDonald, L. W. (eds.), *Color Engineering: Achieving Device Independent Colour*, John Wiley & Sons, England, 127-164.

Berns R. S. and Merrill R. 2002D. Color science and painting. *American Artist*, 68-70, 72, January.

Berns R. S. Taplin, L. A., Imai, F. H., Day, E. A., Day, D. C. 2004D. A comparison of small-aperture and image-based spectrophotometry of paintings. *Studies in Conservation*, submitted.

Berns R. S. Taplin, L. A., Imai, F. H., Day, E. A., Day, D. C. 2004C. Color accurate image archives using spectral imaging. *Proc. National Academy of Sciences*, in press.

Berns, R. S., Byrns, S, Casadio, F., Fiedler, I., Gallagher, C., Imai, F. H., Newman, A., Rosen, M. R., and Taplin, L. A. 2004B. Rejuvenating the appearance of Seurat's *A Sunday on La Grande Jatte – 1884* using color and imaging science techniques – a simulation. Proc. 14th Triennial Meeting The Hague, ICOM Committee for Conservation.

Berns R. S. 2004A. Rejuvenating Seurat's palette using color and imaging science: A simulation. in Herbert, R. L., *Seurat and the Making of La Grande Jatte*, Art Institute of Chicago and University of California Press, 214-227.

Fairman, H. S. 1997. Metameric correction using parametric decomposition. *Color Research and Application* 12, 261-265.

Imai, F. H. 1998. Multi-spectral image acquisition and spectral reconstruction using a trichromatic digital camera system associated with absorption filters. *Munsell Color Science Laboratory Technical Report*,
<http://www.cis.rit.edu/mcsl/research/CameraReports.shtml> and available at
<http://www.art-si.org>.

Imai, F. H., Berns, R. S., and Tzeng, D. 2000A. A comparative analysis of spectral reflectance estimation in various spaces using a trichromatic camera system. *Journal of Imaging Science and Technology* 44, 280-287.

Imai, F. H., Rosen, M. R., and Berns, R. S. 2000B. Comparison of spectrally narrow-band capture versus wide-band with a priori sample analysis for spectral reflectance

estimation. Proc. of the Eighth Color Imaging Conference: Color Science and Engineering, Systems, Technologies and Applications, Society of Imaging Science and Technology, Springfield, VA , 234-241.

Imai, F. H., Taplin, L. A., Day, E. A. 2002. Comparison of the accuracy of various transformations from multi-band images to reflectance spectra. Munsell Color Science Laboratory Technical Report, <http://www.art-si.org> .

ISO 14524. 1999. Photography – Electronic still-picture cameras – Methods for measuring opto-electronic conversion functions (OECFs), International Organization for Standardization, Geneva Switzerland.

ISO 17321-1. 2003, Graphic technology and photography – Colour characterization of digital still cameras (DSCs) – Part 1: Stimuli, metrology, and test procedures (working draft). International Organization for Standardization, Geneva Switzerland.

Liang, J., Saunders, D., Cupitt, J., and Benchouika, M. 2004. A new multi-spectral imaging system for examining paintings. Proc. of the Second European Conference on Color in Graphics, CGIV'2004, Imaging and Vision, Society of Imaging Science and Technology, Springfield, VA, 229-234.

Mohammadi, M., Nezamabadi, M., Berns, R. S., and Taplin, L. A. 2004. Spectral imaging target development based on hierarchical cluster analysis. Proc. Twelfth Color Imaging Conference, Society of Imaging Science and Technology, Springfield, VA, in press.

Ribés, A., Brettel, H., Schmitt, F., Liang, H., Cupitt, J., and Saunders, D. 2003. Color and multispectral imaging with the CRISATEL multispectral system. Proc. PICS Conference, Society of Imaging Science and Technology, Springfield VA, 215-219.

Saunders, D., and Cupitt, J. 1993. Image processing at the National Gallery: The VASARI project. National Gallery Technical Bulletin 14, 72-85.

Vora, P. L. and Trussell, H. J. 1993. Measure of goodness of a set of color scanning filters. Journal of the Optical Society of America A,10, 8-23.

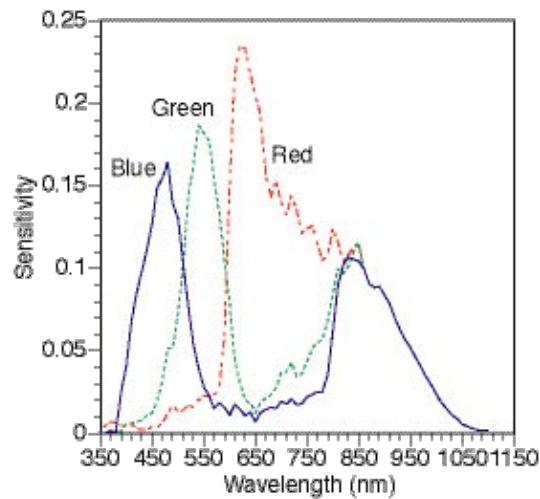


Figure 1. Spectral sensitivities of the Kodak KAF-22000CE color-filter array sensor.

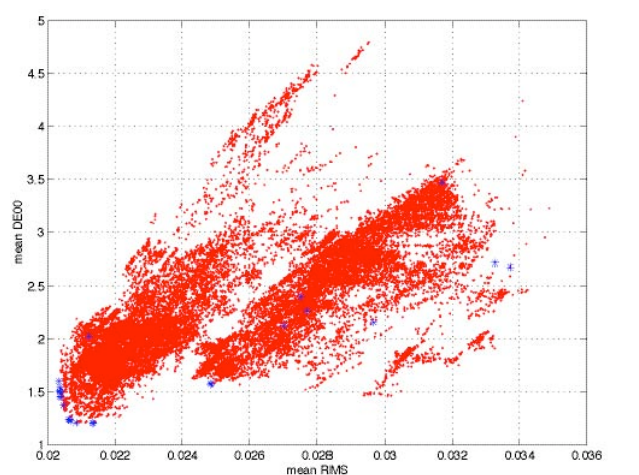


Figure 2. Mean color differences (ΔE_{00} for D65) compared with spectral error, RMS, in the estimation of the Esser calibration target for the selected 30,000 filter pairs. Blue asterisks mark 25 filter pairs selected for further analysis.

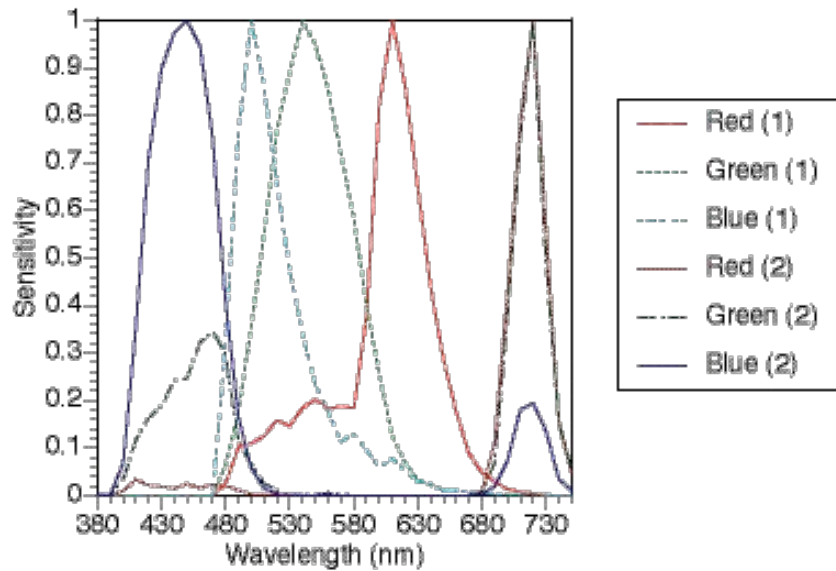


Figure 3. Normalized (by peak height) spectral sensitivities of the modified Sinar 54H.

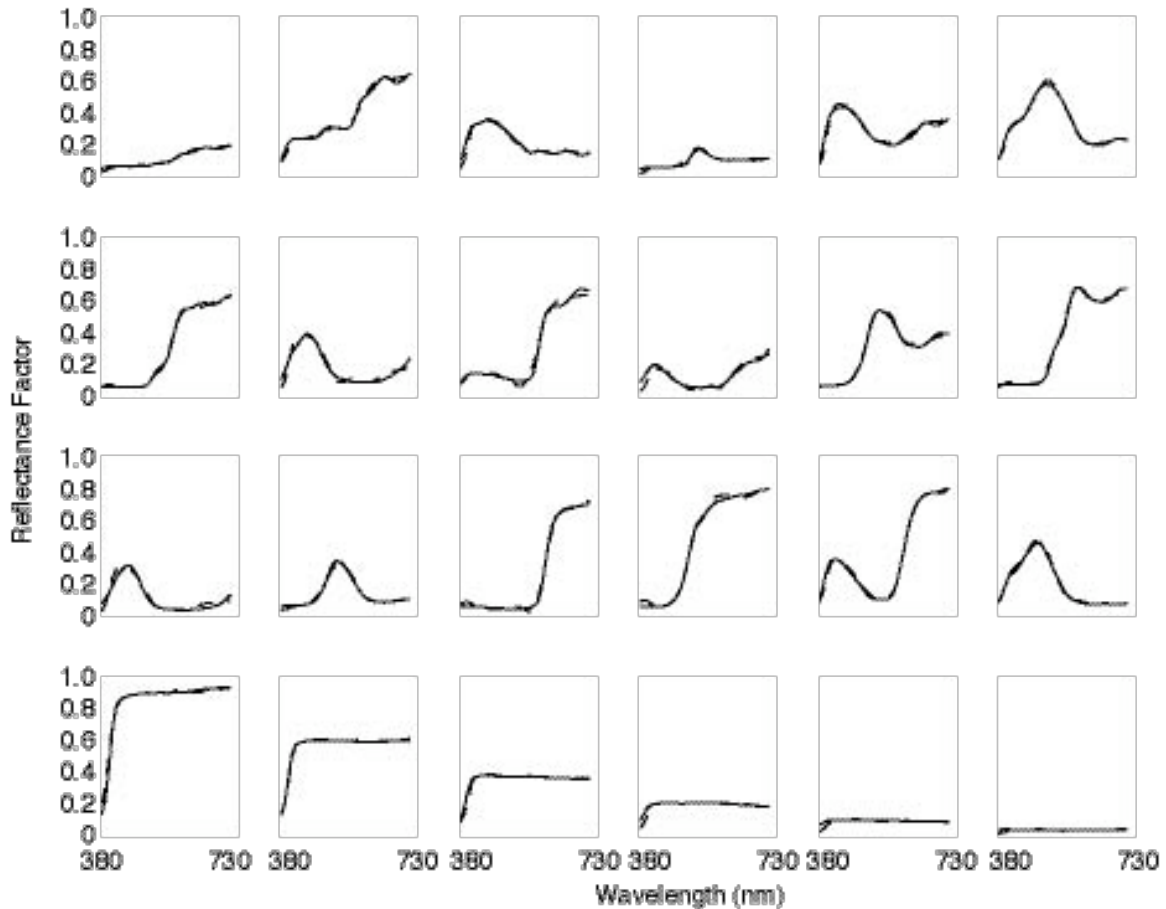


Figure 4. Spectral estimation accuracy of the six-channel modified Sinar54H (dashed line) compared with in situ spectrophotometry (solid line) of the GretagMacbeth ColorChecker.

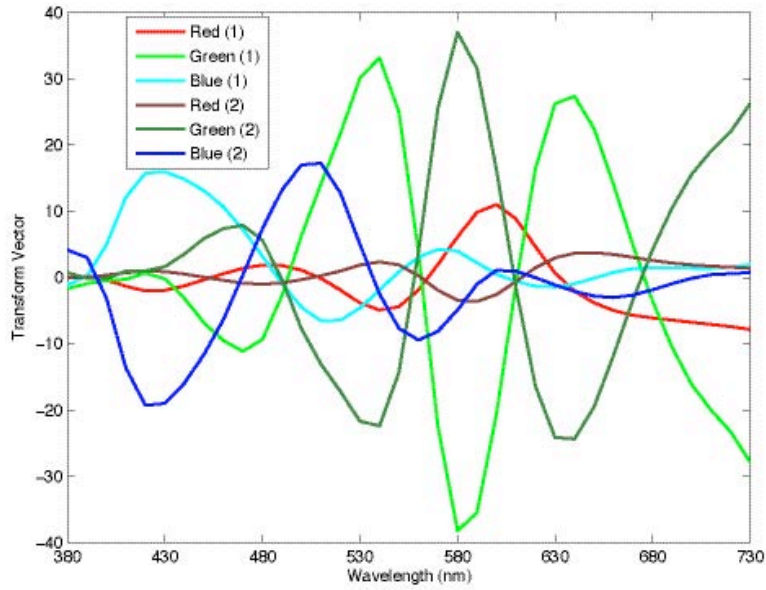


Figure 5 Transform vectors from camera signals to spectral reflectance, \mathbf{M}_s .

Tables

Table I. μ -factor values for each listed combination of taking and rendering illuminants for a production Sinar 54H, the six-channel modified Sinar, and a theoretical camera with spectral sensitivities equal to color-matching functions.

	Production Sinar	Modified 6-channel Sinar	Colorimetric camera
Taking / rendering illuminant			
Tungsten / D65	0.75	0.95	0.96
HMI / D65	0.68	0.73	0.53
D65 / D65	0.85	0.96	1.00

Table II. Performance metrics comparing a conventional small-aperture in situ spectrophotometer with the “production” Sinarback 54H colorimetric image for the calibration (ColorChecker DC) and verification data (ColorChecker) using Eq. (5).

ΔE_{00}	ColorChecker	
	DC	ColorChecker
Mean	1.9	2.6
Max	10.9	9.2
Std. Dev.	1.9	2.0

Table III. Performance metrics comparing a conventional small-aperture in situ spectrophotometer with the modified Sinarback 54H spectral image for the calibration (ColorChecker DC) and verification data (ColorChecker) using Eq. (4).

	ΔE_{00} (D65, 2°)	RMS (%)	Metameric Index (D65 -> A, ΔE_{00})	Metameric Index (A -> D65, ΔE_{00})
ColorChecker DC				
Average	1.4	1.6	0.5	0.6
Maximum	13.3	4.0	5.0	6.5
Std. Dev.	1.6	0.6	0.8	0.9
ColorChecker				
Average	1.2	1.6	0.3	0.4
Maximum	3.5	2.6	1.4	1.7
Std. Dev.	0.9	0.6	0.4	0.4

Table IV. Performance metrics comparing a conventional small-aperture in situ spectrophotometer with the modified Sinarback 54H spectral image for the calibration (ColorChecker DC) and verification data (ColorChecker) using Eqs. (4) and (5).

	ΔE_{00} (D65, 2°)	RMS (%)	Metameric Index (D65 -> A, ΔE_{00})	Metameric Index (A -> D65, ΔE_{00})
ColorChecker DC				
Average	0.9	1.5	0.5	0.6
Maximum	3.0	3.9	5.0	5.9
Std. Dev.	0.7	0.6	0.8	0.8
ColorChecker				
Average	0.9	1.6	0.3	0.4
Maximum	2.2	2.6	1.4	1.5
Std. Dev.	0.5	0.6	0.4	0.4